ELSEVIER

Journal of Alloys and Compounds 446–447 (2007) 368–372

Journal of ALLOYS AND COMPOUNDS

www.elsevier.com/locate/jallcom

Inelastic neutron scattering of H_2 adsorbed on boron substituted single walled carbon nanotubes

Y. Liu [a,b], C.M. Brown [b,c,*], J.L. Blackburn [d], D.A. Neumann [b], T. Gennett [d], L. Simpson [d], P. Parilla [d], A.C. Dillon [d], M.J. Heben [d]

[a] *Department of Materials and Engineering, University of Maryland, College Park, MD 20742, USA*
[b] *NIST Center for Neutron Research, 100 Bureau Drive, Gaithersburg, MD 20899-8562, USA*
[c] *Indiana University Cyclotron Facility, Indiana University, 2401 Milo B. Sampson Lane, Bloomington, IN 47408, USA*
[d] *Center for Basic Science, National Renewable Energy Laboratory, 16253 Denver West Parkway, Golden, CO 80401, USA*

Received 30 October 2006; received in revised form 11 January 2007; accepted 11 January 2007
Available online 25 January 2007

Abstract

We report inelastic neutron scattering investigations of hydrogen adsorbed on both purified boron substituted (≤1%) single walled carbon nanotube bundles and purified single walled carbon nanotube bundles. Samples of both types were generated by both arc and laser production methods. At H_2 coverages ≤3 H_2/B, a clear splitting is observed for the H_2 rotation transition peak at about 14.7 meV in all arc-produced samples. In contrast, the spectra from laser-produced materials exhibit one broad peak. Further increase in H_2 coverage results in adsorption at lower binding energy sites. No distinct signature of an enhanced boron–hydrogen interaction is observed. However, the overall line width of the rotation transition peak from a laser-produced sample is substantially smaller than that from arc-prepared samples. This difference might imply that some features of the H_2 rotation transition peak might not be due to the intrinsic features of single wall carbon nanotubes.
Published by Elsevier B.V.

Keywords: Energy storage materials; Hydrogen storage materials; Nanostructured materials; Neutron scattering

1. Introduction

Carbon is a light element, able to be produced in large quantities with very high specific surface areas at relatively low cost. Therefore, interest in moving to a hydrogen-based economy, along with early reports of as much as 10 wt% hydrogen reversibly stored on single walled carbon nanotubes (SWNTs) [1], has led to widespread interest in the possibility of using nanoporous carbons as a medium for solid-state hydrogen storage. However, there now seems to be a consensus forming that if carbon is going to be technologically useful in storing hydrogen, methods must be developed to enhance the binding energy of H_2 to the carbon framework, while maintaining the high specific surface area. Two recently proposed approaches that could increase the interaction of hydrogen with carbons are decorating the material with metal catalysts [2,3] and substituting boron for carbon [4]. Neutron scattering has previously been used to probe the local potential at a physisorption site via the rotational transition of molecular hydrogen [5–8]. Our initial study of hydrogen physisorbed on bundles of laser-produced, un-purified, nanotubes produced a spectrum that was considerably broadened from a nominally resolution limited rotational peak that was only slightly reduced from the free rotor valve of 14.7 meV [5]. Subsequently data for as-prepared arc-produced materials were presented [6] and then reinterpreted and somewhat expanded [7], with a clear multi-peaked feature being rationalized in terms of the hydrogen experiencing a stronger rotational hindering potential in what is most likely the groove sites as compared to hydrogen on the exterior surfaces of the bundles. Similar multi-peak inelastic features were also seen for a carbon sample produced by decomposition of $Fe(CO)_5$ in a CO environment (HiPCo) [8].

In this paper, we present inelastic neutron scattering results of the rotational spectra from hydrogen adsorbed upon carbon nanotube materials synthesized with the aim of increasing the

* Corresponding author at: Indiana University Cyclotron Facility, Indiana University, 2401 Milo B. Sampson Lane, Bloomington, IN 47408, USA.
Tel.: +1 301 975 5134; fax: +1 301 921 9847.
E-mail address: craig.brown@nist.gov (C.M. Brown).

0925-8388/$ – see front matter. Published by Elsevier B.V.
doi:10.1016/j.jallcom.2007.01.113

binding potential by the incorporation of boron into the nanotube lattice. Additionally, we call into question the assignment of hydrogen adsorption at the groove sites as the origin of the splitting of the rotational transition for arc-produced samples.

2. Experimental details

Carbon nanotubes and boron substituted carbon nanotube samples were prepared by both the arc discharge and the laser ablation methods.

C-SWNTs were produced from graphite targets having ≈0.6 at.% each of Ni and Co powders. B-SWNTs were produced from graphite targets having 11 at.% nickel boride (NiB) [9]. The carrier gas for all laser syntheses was nitrogen, as it was found that nitrogen allows for higher B doping levels than argon [9]. The furnace temperature during synthesis was 1175 °C. Samples were vaporized with a pulsed YAG or alexandrite laser, with power densities of ≈45–65 W/cm^2.

The first step in arc synthesis is packing a pre-bored consumable graphite rod with a graphite/catalyst powder. The catalyst mixture for the C-SWNTs was graphite (Alfa-Aesar, 2–7 μm) [10] doped with Ni and Co in concentrations of 0.6 at.% each. The catalyst mixture for the B-SWNTs contained 0.3 at.% Ni and Co, and 6 at.% NiB. A helium flow rate of 500 standard cm^3/min was maintained over the course of the experiments with a constant pressure of 0.667 bar. The power supply was set to allow for the flow of a constant 70–110 A at 20 V for the arc struck between the consumable and stationary rods.

Raw laser soots were purified in a similar manner to that reported previously [11]. Briefly, ≈100 mg of raw soot was refluxed in 180 mL of 3 mol/L nitric acid for 16 h. The material was filtered, washed with water several times, and then washed successively with acetone and water until the filtrate became clear. Finally, the sample was washed with ≈15 mL of 1 mol/L potassium hydroxide, followed by water until the filtrate became clear. The resulting paper was oxidized in static air at 500–520 °C. Further metal extraction was done by placing the resulting SWNT paper in concentrated hydrochloric acid for several hours followed by washing with water and 1 M potassium hydroxide. The paper was then heated in flowing carbon dioxide to 800 °C for 1 h. Two more HCl extractions followed by carbon dioxide treatments were then performed.

The purification method was modified for the arc soot because it was found that the arc samples do not typically survive the 16 h reflux in 3 mol/L nitric acid. This is likely due to the presence of more defects on these arc-prepared SWNTs. Raw arc mats were first heated in flowing carbon dioxide at 800 °C for 15 min, followed by a concentrated HCl extraction for ∼4 h. The SWNT mats were then washed with water and potassium hydroxide as described above. Finally, the washed mats were heated in carbon dioxide at 800 °C for 1 h. The HCl extraction, washing, and 1 h carbon dioxide treatments were then repeated two more times.

Raman spectroscopy was performed using 3–4 mW of a 488 nm laser excitation [9] in the back-scattering configuration.

Hydrogen gas isotherms were measured on a volumetric Sieverts apparatus specifically designed for small sample masses [12]. Samples (5–70 mg) were placed into platinum foils and weighed before being placed into a quartz tube and loaded onto the volumetric apparatus. A Mettler-Toledo UMT2 microbalance [10] with a readability of 0.1 μg and a repeatability of 0.25 μg was used to determine the weight of each sample which was weighed three times. The sample tube was evacuated to a base pressure of ≈1×10^{-4} Pa before loading with helium or hydrogen. Helium was used to measure the free volume of the sample compartment, and single point hydrogen adsorption measurements were performed at several different hydrogen pressures at a temperature of 77 K.

Prompt-γ activation analysis (PGAA) was performed at the National Institute of Standards and Technology Center for Neutron Research (NCNR) [13]. Boron substituted samples were packaged in aluminum foil and suspended in the white neutron beam. Integrated count rates for the characteristic lines of carbon, boron, nickel and cobalt were compared to those of standard samples to obtain atomic ratios. Measurements of the PGAA spectrum of the aluminum foil showed that there was no contamination of the peaks of interest for the nanotube samples from the sample holder.

Inelastic neutron spectra were collected using the Filter Analyzer Neutron Spectrometer (FANS) at the NCNR. A pyrolytic graphite monochromator coupled with two 20′ collimators was used to tailor the incident beam. After scattering from the sample, a filter consisting of room temperature bismuth and cryogenically cooled beryllium–graphite was used to select the final neutron energy [14]. The samples were packaged in aluminum foil and mounted in an aluminum cell equipped with a packless valve able to be attached to a stainless steel gas fill line in a modified closed cycle refrigerator. The samples were degassed overnight at 473 K with a dynamic vacuum provided by a turbopump. Background data were recorded for all samples at a temperature of 3.5 K while under vacuum. Hydrogen dosing of the samples was performed with the temperature of the sample above 70 K. The sample was then cooled at a rate of ≈1 K/min, after which a 30 min equilibration was allowed before measuring any spectrum. Measurements were taken at a given H_2:B ratio for each of the arc and laser B-SWNT samples. Due to the different boron concentrations in the samples, a 1 H_2:B loading for the arc sample corresponds to a mass fraction of 0.1%, while for the laser sample it corresponds to mass fraction of 0.2%. The C-SWNT samples were loaded with the equivalent hydrogen contents by scaling to the mass of the sample.

3. Results and discussion

The overall sample purity for the laser-produced C-SWNTs is higher than that of the laser-produced B-SWNTs due to residual metal particles encapsulated in multi-walled graphitic cages [9]. The so-called D band of the Raman spectra at ≈1340 cm^{-1} arises from both carbonaceous impurities (*i.e.* amorphous carbon), as well as defects on the SWNTs themselves [15,16]. Graphitic impurities do not affect the intensity or structure of this band. The lower intensity, structured D band for the laser-produced B-SWNTs results from both a lower defect density than the arc-produced B-SWNTs and a lower level of amorphous impurities as a result of the more rigorous purification process. The D bands for arc-produced SWNT are similar amongst themselves, and likewise for the laser-produced SWNTs, indicating similar levels of defect densities arise from the production method of choice.

Raman spectra taken in the region of the diameter-dependent radial breathing mode consistently displayed a higher energy feature for the arc-produced B-SWNTs (≈194 cm^{-1}) than those from C-SWNTs (≈174 cm^{-1}). This implies that the boron catalyst promotes the formation of smaller diameter SWNTs in the arc system. This variation in the average diameter as a function of boron doping is not seen for the laser-produced SWNTs [9], although variations in the average diameter may occur for either B-SWNTs or C-SWNTs as a function of laser power [17,18].

The results of the prompt-γ activation analysis are presented in Table 1. Whilst this data does not give specific bonding information between the carbon and boron, it does provide a sensitive determination of the bulk composition of the sample. We find that there is approximately half the boron content in the arc-produced B:SWNT sample (B:C = 0.006(1)) as compared to

Table 1
PGAA of B:SWNT and SWNT samples prepared by the arc discharge and laser methods

Sample	B:C (×10^2)	Ni:C (×10^2)	Co:C (×10^2)
B:SWNT (laser)	1.2(1)	1.2(1)	–
B:SWNT (arc)	0.6(1)	0.4(1)	0.04(1)
SWNT (laser)	$1.0(2) \times 10^{-2}$	0.06(1)	0.05(1)
SWNT (arc)	$<3 \times 10^{-3}$	0.6(1)	0.6(1)

Relative atom ratios of selected elements to carbon are multiplied by 100 to give approximate atom percent compositions. Estimated standard deviations are based on counting statistics and given in parentheses.

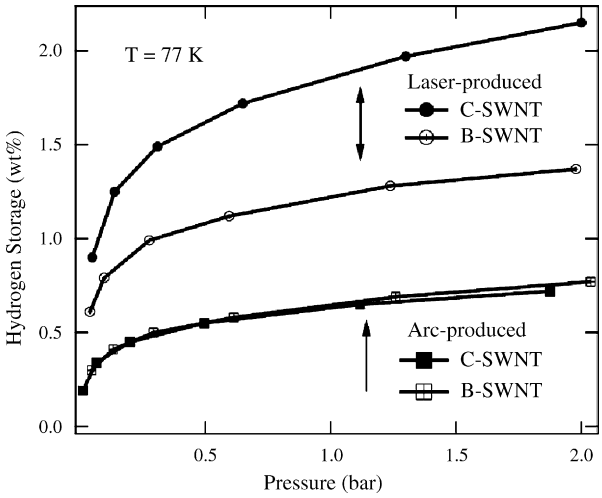

Fig. 1. Comparison of volumetric hydrogen storage capacities of laser-produced and arc-produced C-SWNTs and B-SWNTs.

the laser-produced sample (B:C = 0.012(1)). These data agree well with previous results [9] where boron incorporation for the laser-produced B-SWNTs was analyzed by nano-probe electron energy loss spectroscopy (EELS). Substitutional boron incorporation at levels of 1.0–1.7 at.% was found for SWNTs in the raw soot produced with the NiB catalyst and was reduced to ~0.5–1.0 at.% for the purified laser-produced B-SWNTs. EELS measurements on arc-produced B-SWNTs have not yet been performed. However, we have discovered some characteristic variations in the absorbance and Raman spectra of SWNTs dispersed in surfactant solutions that arise from boron doping [18]. These variations include an apparent enhancement in the absorption coefficient for the B-SWNTs, as well as modification of the features in the Raman spectra which are dominated by scattering from metallic SWNTs. These variations occur in both the laser-produced and arc-produced SWNTs, and serve as another tool by which we may infer that boron incorporation of similar levels (≈0.5–1.0%) is achieved for the arc-produced SWNTs, in agreement with the other data presented here.

Relative ratios of cobalt and nickel catalyst for the bulk samples are given in Table 1. There is much less cobalt in the final purified products compared to the initial metal concentrations in the arc rods. In contrast the nickel component in the purified arc material is only somewhat reduced in the C-SWNT, while it is much reduced in the B-SWNT materials. For the laser materials, the catalyst is reduced by an order of magnitude from the initial composition, yet there is still twenty times more residual catalyst in the B-SWNTs.

Fig. 1 compares the volumetric hydrogen storage capacities of laser and arc-produced C-SWNTs and B-SWNTs. The differences in the hydrogen storage capacities are likely a reflection of the overall sample purity. For example, the laser-produced C-SWNT storage capacity is ≈50% higher than the laser-produced B-SWNTs because of the afore-mentioned graphite-encapsulated metal impurities in the latter. Unfortunately, this difference in sample purity will mask any difference in adsorption capacity that results from boron doping though more careful measurements at lower pressures, where any boron effect is expected to be most evident, are under way. We are also working on methods to remove these graphite-encapsulated metal impurities. Both of the laser-produced samples have significantly higher storage capacities than the arc-produced samples possibly due to the more rigorous purification process for the laser-produced samples. As discussed above, this difference in purity is also reflected in the D band of the Raman spectrum [9,16] and the PGAA results.

In contrast to the laser-produced samples, the difference in the storage capacity between arc-produced C-SWNTs and B-SWNTs is minimal. This is due, in part, to the fact that the arc process does not produce graphite-encapsulated metal particles when boron is doped into the target mixture. The lack of graphite-encapsulated particles means that the purification process is equally effective for both undoped and doped arc samples. The fact that the isotherms for the arc-produced samples are essentially identical implies that any effect of boron doping on the hydrogen storage capacity is not observable with this technique for our samples. This is likely due to the very low B doping levels achieved at this point.

Neutron scattering can be used as a local probe of the hydrogen adsorption sites through the strong frequency dependence of the rotational transition upon the rotational barrier. This rotational barrier will cause the rotation transition peak of H_2 (≈14.7 meV) to split into two or three peaks. Different rotation barriers due to different binding sites will cause different splitting features, from which one can indirectly probe these binding sites.

Fig. 2 (left panel) shows the neutron spectra as a function of hydrogen loading of both arc-produced C-SWNT and B-SWNT samples, along with (right panel) the difference spectra between loadings. For both B- and C-SWNT samples, one observes very similar spectra that are at least doublets for loading level above the 0.5 H_2:B. These spectra can be fitted to two Gaussian peaks and one obtains peak positions similar to those observed by others for as-prepared SWNTs [6–8], at 13.5 and 15.1 meV, but not by us for laser prepared materials [5]. Even though the peaks for the B-SWNT material seem to be very slightly broader than those from the C-SWNTs, there are no major differences in the spectra that could be interpreted as arising from a significant increasing in the hydrogen binding potential. One could consider this as being due to the boron doping level being small and the majority of the boron, if randomly distributed through the tubes and hence the bundles, being inaccessible to hydrogen. More experiments are needed to address this issue. The difference spectra indicate that the two main peaks grow at different rates with higher loading. This may be due to the emergence of the essentially unhindered 14.5 meV rotor line as described by the higher resolution studies. In this experiment, this occurs for the 0.2 mass fraction of hydrogen loading while it only appears strongly above 50% hydrogen monolayer coverage, or about 0.55 mass fraction, for the as-prepared arc samples [6]. However, a direct comparison between materials is somewhat difficult due to the different catalyst, amorphous carbon and nanotube contents between samples.

Fig. 3 displays the corresponding data for the laser B- and C-SWNTs with approximately double the hydrogen loaded per

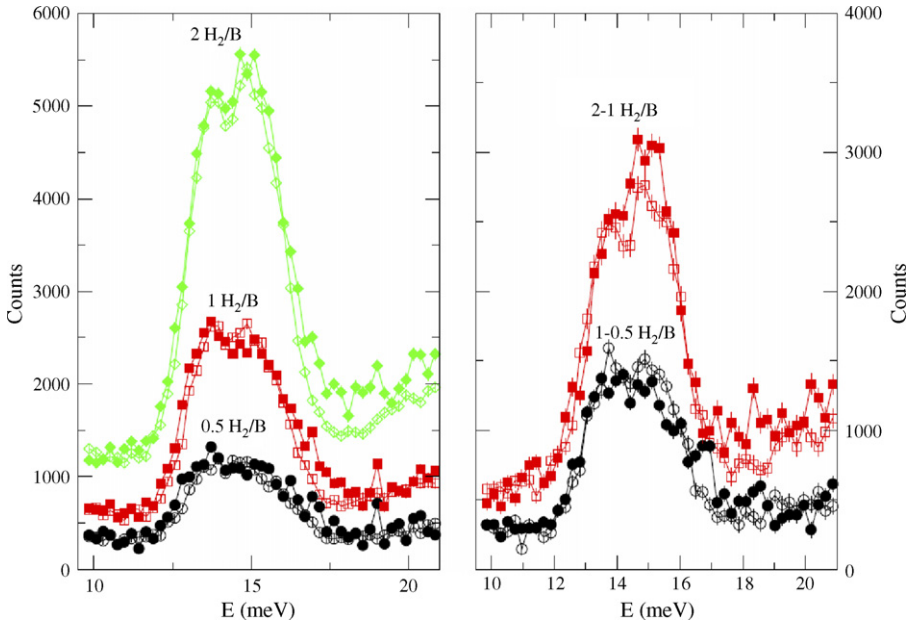

Fig. 2. Neutron spectra for arc-produced C-SWNT (empty symbols) and B-SWNTs (filled symbols). A mass fraction of 0.1% is equivalent to 1 H_2:B atomic ratios of the B-SWNT samples are. Right panel displays the difference spectra indicated. One standard deviation error bars are based on counting statistics.

unit mass as compared to the arc samples. Again, there are no extra peaks that can be attributed to the expected boron effect. Experiments are on-going to understand the slightly different peak shape at 1 and 2 H_2/B. Upon hydrogen loading the 14.5 meV peak grows. The spectra are much narrower than their arc counterparts and are similar to the spectra obtain previously for as-prepared C-SWNTs [5].

While our initial study [5] was performed on the same spectrometer as this study, which has a resolution of 1.1 meV, the spectrometer used for the other two studies were performed on has better resolution (0.3 meV) [6–8]. However, it is clear that the spectrometer used here is able to resolve the main peaks at 13.5 and 15.1 meV and hence observe the so-called groove sites if they were present in the laser-produced materials. The question then arises as to the true origins of the split rotational peaks in the arc and HiPCo samples. The fact that the characteristics of this feature remain similar between samples, despite the change in average tube radii, also adds credence to the supposition that

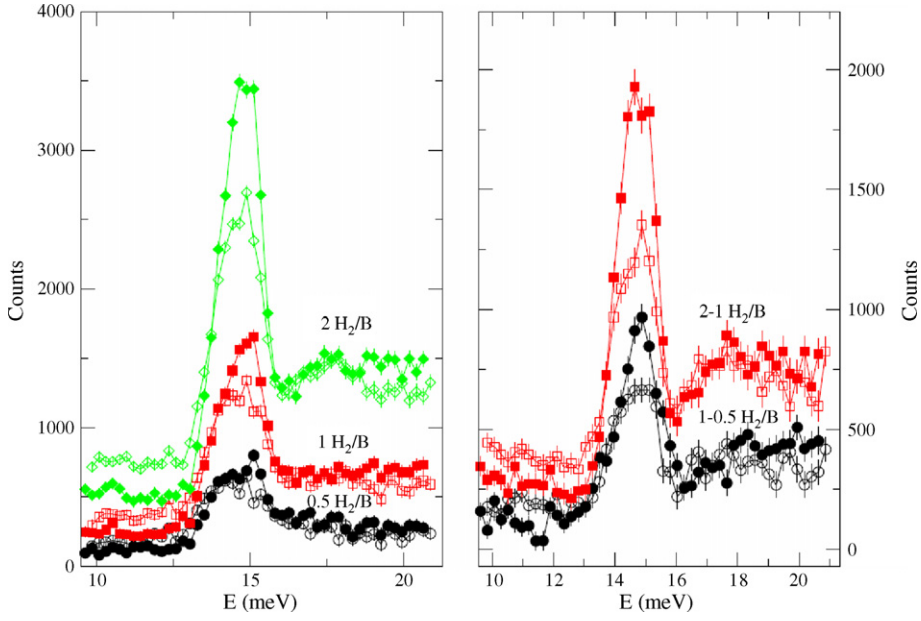

Fig. 3. Comparison of neutron spectra for laser-produced C-SWNT (empty symbols) and B-SWNTs (filled symbols). Data are labeled for H_2:B atomic ratios of the B-SWNT samples with the equivalence of 0.2% mass fraction being equivalent to 1 H_2. Right panel displays the difference spectra between 0.5 H_2:B and 1 H_2:B and 1 H_2:B and 2 H_2:B. One standard deviation error bars are based on counting statistics.

it may not be an intrinsic feature of a bundle of pristine nanotubes. Still, we cannot rule out a lifting of the symmetry and a splitting within the observed broad peak of the laser-produced samples. There are two major differences between the typical arc and laser bundles: one is the increased defect density present in the arc samples and a much weaker resistance to acids; the other is the average distribution of chirality/radii as measured by electron diffraction [19]. A typical bundle of laser-produced nanotubes is composed of a bundle of five or so smaller bundles each with uniform chirality whilst the average arc-produced bundle is comprised of a much broader distribution of nanotubes. The defects or imperfections in the nanotubes themselves would then be the logical source of the disparity between the hydrogen rotational spectra. We are currently attempting to confirm this speculation.

4. Conclusions

We have measured the rotational spectra of hydrogen molecules adsorbed on purified laser-produced and arc-produced single walled nanotube bundles and their boron substituted counterparts using inelastic neutron scattering. The expected larger binding potential for hydrogen at low-loading on the boron substituted samples was not observed and may reflect the low boron concentrations. Spectra of the arc-produced samples resemble those published by others [6–8], while the laser materials resemble our previous work [5]. We have shown that the arc materials and the laser-produced materials have somewhat different hydrogen binding sites and propose that this stems from sample purity or imperfection and defects of the tubes.

Acknowledgements

This work was partially supported by the US Department of Energy's Office of Energy Efficiency and Renewable Energy within the Center of Excellence on Carbon-based Hydrogen Storage Materials.

References

[1] A.C. Dillon, K.M. Jones, T.A. Bekkedahl, D.S. Bethune, M.J. Heben, Nature 386 (1997) 377.
[2] Y.F. Zhao, Y.H. Kim, A.C. Dillon, M.J. Heben, S.B. Zhang, Phys. Rev. Lett. 94 (2005) 15504.
[3] T. Yildirim, S. Ciraci, Phys. Rev. Lett. 94 (2005) 175501.
[4] Y.-H. Kim, Y. Zhao, A. Williamson, M.J. Heben, S.B. Zhang, Phys. Rev. Lett. 96 (2006) 016102.
[5] C.M. Brown, T. Yildirim, D.A. Neumann, M.J. Heben, T. Gennet, A.C. Dillon, J.L. Alleman, J.E. Fischer, Chem. Phys. Lett. 329 (2000) 311.
[6] P.A. Georgiev, D.K. Ross, A. De Monte, U. Montaretto-Marullo, R.A.H. Edwards, A.J. Ramirez-Cuesta, D. Colognesi, J. Phys.: Condens. Matter 16 (2004) L73.
[7] P.A. Georgiev, D.K. Ross, A. De Monte, U. Montaretto-Marullo, R.A.H. Edwards, A.J. Ramirez-Cuesta, M.A. Adams, D. Colognesi, Carbon 43 (2005) 895.
[8] H.G. Schimmel, G.J. Kearley, F.M. Mulder, Chem. Phys. Phys. Chem. 5 (2004) 1053.
[9] J.L. Blackburn, Y. Yan, C. Engtrakul, P.A. Parilla, K. Jones, T. Gennett, A.C. Dillon, M.J. Heben, Chem. Mater. 18 (2006) 2558.
[10] Certain commercial materials and equipment are identified in order to specify adequately experimental procedures. In no case does such identification imply recommendation or endorsement by the National Institute of Standards and Technology, nor does it imply that the items identified are necessarily the best available for the purpose.
[11] A.C. Dillon, T. Gennett, K.M. Jones, J.L. Alleman, P.A. Parilla, M.J. Heben, Adv. Mater. 11 (1999) 1354.
[12] M.J. Heben, A.C. Dillon, K.E.H. Gilbert, P.A. Parilla, T. Gennett, T.J.L. Alleman, G.L. Hornyak, K.M. Jones, Hydrogen Mater. Vac. Syst. (2003) 77.
[13] R.L. Paul, R.M. Lindstrom, A.E. Heald, Radioanal. Nucl. Chem. 215 (1997) 63.
[14] T.J. Udovic, D.A. Neumann, J. Leao, C.M. Brown, Nucl. Instrum. Meth. A517 (2004) 189.
[15] A.C. Dillon, P.A. Parilla, J.L. Alleman, T. Gennett, K.M. Jones, M.J. Heben, Chem. Phys. Lett. 401 (2005) 522.
[16] A.C. Dillon, M. Yudasaka, M.S. Dresselhaus, J. Nanosci. Nanotechnol. 4 (2004) 691.
[17] A.C. Dillon, P. Parilla, J.L. Alleman, J.D. Perkins, M.J. Heben, J. Chem. Phys. Lett. 316 (2000) 13.
[18] J.L. Blackburn, C. Engtrakul, T.J. McDonald, A.C. Dillon, M.J. Heben, J. Phys. Chem. B 110 (2006) 25551.
[19] J.-F. Colomer, L. Henrard, Ph. Lambin, G. Van Tendeloo, Eur. Phys. J. B 27 (2002) 111.